

Experimental and numerical study of scour downstream Toachi Dam

Luis G. Castillo

Hidr@m Group, Civil Engineering Department, Universidad Politécnica de Cartagena, Spain

Marco Castro

Centro de Investigaciones y Estudios en Recursos Hídricos (CIERHI), Escuela Politécnica Nacional, Ecuador

José M. Carrillo

Hidr@m Group, Civil Engineering Department, Universidad Politécnica de Cartagena, Spain

Daniel Hermosa, Ximena Hidalgo & Patricio Ortega

Centro de Investigaciones y Estudios en Recursos Hídricos (CIERHI), Escuela Politécnica Nacional, Ecuador

ABSTRACT: The study analyzes the expected changes in the Toachi River (Ecuador) as a result of the construction of the Toachi Dam (owned by CELEC EP Hidrotoapi). Toachi is a concrete dam with a maximum height of 59 m to the foundations. The top level is located at an altitude of 973.00 meters above sea level. With normal maximum water level located at 970.00 m, the reservoir has a length of 1.30 km in the Sarapullo River and 3.20 km in the Toachi River. The dam has a free surface weir controlled by two radial gates. It consists in 2 channels located in center of the dam that end in ski jump. The discharge is controlled by radial gates in order to ensure the accurate operation in the event when the gates are partially open. The spillway has been designed to spill up to a rate flow of 1213 m³/s. It is necessary to know the shape and dimensions of the scour generated downstream of the dam. This scour is studied with four complementary procedures: laboratory model with 1:50 Froude scale similitude, empirical formulae obtained in models and prototypes, semi-empirical methodology based on pressure fluctuations-erodibility index, and Computational Fluid Dynamics (CFD) simulations.

1 DAM CHARACTERISTICS

The Toachi Dam is located in the South-West of the Quito city (Ecuador). It is a concrete dam with a maximum height of 59 m to the foundations. The top level has a length of 170.5 m and 10 m of thickness. It is located at an altitude of 973 meters above the sea level. The upstream and downstream embankment side slopes are 0.3/1.0 and 0.7/1.0 (horizontal/vertical), respectively.

The reservoir collects water from the basins of the Toachi and Sarapullo rivers. It has a total volume of 8 Hm³ with normal maximum water level located at 973 meters. At this level, the reservoirs have a length 1.3 km in the Sarapullo River and 3.2 km in the Toachi River.

The dam has two Creager spillways controlled by gates. The spillways end in a ski jump and they have two baffles to divide the flow. The design flow matches a 1000 years return period (1213 m³/s) with an energy head of 7.50 m. There are two bottom outlets whose capacity is 800 m³/s. The dam also has a stepped spillway for the Sarapullo River with a design flow of 40 m³/s (Figure 1).

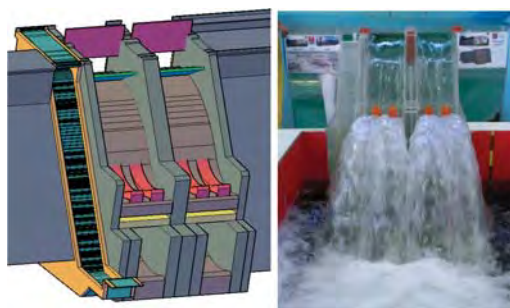


Figure 1. Three-dimensional view and physical model of the Toachi Dam.

2 PHYSICAL MODEL

The physical model was built with a Froude scale 1:50 in the Centro de Investigaciones y Estudios en Recursos Hídricos (CIERHI) of the Escuela Politécnica Nacional (Ecuador). The scour downstream the dam was analyzed by using different flows according

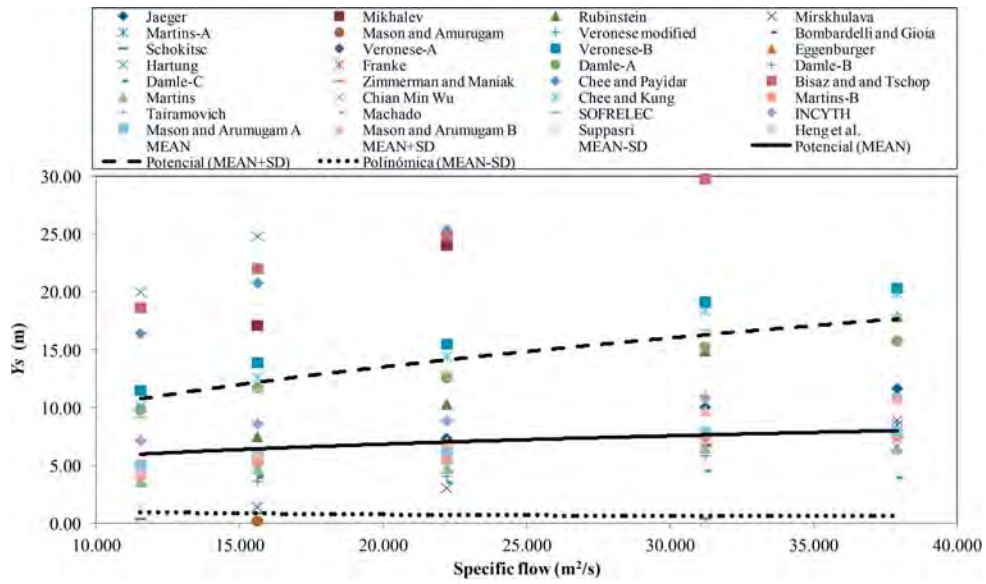


Figure 4. Scour of the ski jump obtained with 30 formulae and the threshold of ± 1 standard deviation.

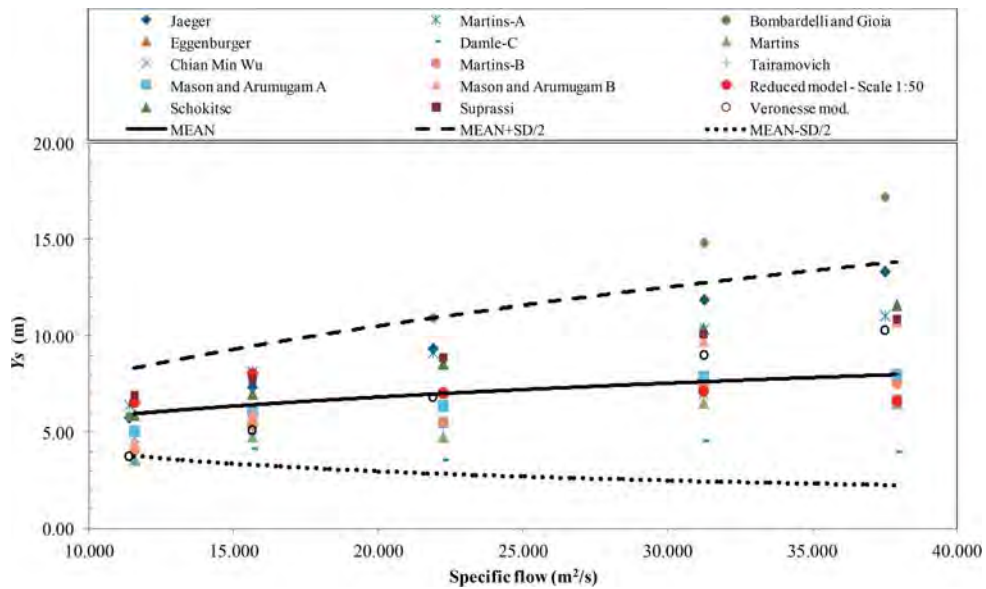


Figure 5. Scour of the ski jump obtained with the formulae in the threshold of ± 0.50 standard deviation.

Table 2. Four scour general formulae with values that fall in the mean value ± 1 standard deviation.

Author	Year	Equation
Jaeger	1939	$D_S = 0.6q^{0.5}H^{0.25}(h/d_m)^{0.333}$
Martins-A	1973	$\begin{cases} D_S = 0.14N - 0.73\frac{h^2}{N} + 1.7h. \\ N = (Q^3H^{1.5}/d_m^2)^{1/7} \end{cases}$
Veronese modified	1994	$D_S = 1.90h^{0.225}q^{0.54}\sin\theta_T$
Bombardelli & Gioia	2006	$D_S = K\frac{q^{0.67}H^{0.67}}{g^{0.33}d^{0.33}}\left(\frac{\rho}{\rho_s - \rho}\right)$

Table 3. Coefficients of five scour simplified formulae with values that fall in the mean value ± 1 standard deviation.

Author	Year	<i>k</i>	<i>a</i>	<i>b</i>	<i>c</i>	<i>d</i>	<i>e</i>	<i>f</i>	<i>h</i>	<i>i</i>
Tairamovich	1978	0.633	0.67	0.25	0	0	0	0	0	0
Martins-B	1975	1.50	0.60	0.10	0	0	0	0	0	0
Mason-Arumugam A	1985	3.27	0.60	0.05	0.15	0	0.30	0.10	0	0
Damle-C	1966	0.362	0.50	0.50	0.50	0	0	0	0	0
INCYTH	1981	1.413	0.50	0.25	0	0	0	0	0	0

Table 4. Erodibility index parameters (Adapted from Annandale, 2006).

Material	Formulae	Parameters
Rock	$M_s = 0.78C_r UCS^{1.05} \text{ when } UCS \leq 10MPa$ $M_s = C_r UCS \text{ when } UCS > 10MPa$ $C_r = g\rho_r/\gamma_r$	UCS = unconfined compressive strength C_r = coefficient of relative density ρ_r = mass density of the rock g = gravitational acceleration γ_r = reference unit weight of rock ($27 \cdot 10^3$ N/m ³)
Non-cohesive granular soil	The relative magnitude is obtained by means of the standard penetration test (SPT). When the SPT value exceeds 80, the non-cohesive granular material is taken as rock.	RQD = rock quality designation RQD = values range between 5 and 100
Rock	$K_b = RQD/J_n$	J_n = values range between 1 and 5 K_b = values range between 1 and 100 J_n = joint set number
Non-cohesive granular soil	$K_b = 1000d^3$	d = characteristic particle diameter (m)
Rock	$K_d = J_r/J_a$	J_r = joint wall roughness number J_a = joint wall alteration number

of the jet flight, diameter (circular jet) or thickness (rectangular jet) in impingement jet conditions and water cushion depth.

Annandale (1995, 2006) summarized and established a relationship between the stream power and the erodibility index for a wide variety of materials and flow conditions. The stream power per unit of area available of an impingement jet is:

$$P_{jet} = \frac{\gamma QH}{A} \tag{2}$$

where γ is the specific weight of water, Q the flow, H the drop height, and A the jet area on the impact surface. The jet area was estimated using the equations of the impingement jet thickness for the free falling jet case (Castillo *et al.*, 2014b and 2015b), in which the throwing distance and the specific flow are considered.

The impingement jet thickness formula has been obtained as:

$$B_j = B_g + 2\xi = \frac{q}{2gH} + 4\varphi h(2H - 2h) \tag{3}$$

where B_g is the thickness due to gravity effect, ξ the jet lateral spread distance due to the turbulence

effect, q the specific flow, H the fall height, and h is the energy head at the crest weir. $\varphi = K_\varphi T_u$, being T_u the turbulence intensity, and K_φ an experimental parameter (1.14 for circular jets and 1.24 for the three-dimensional nappe flow case).

The erodibility index (Annandale, 2006) is defined as:

$$K = M_s K_b K_d J_s \tag{4}$$

being M_s the number of resistance of the mass, K_b the number of the block size, K_d the number of resistance to shear strength on the discontinuity contour, and J_s the number of structure relative of the grain. Table 4 shows the formulae of the parameters.

The threshold of rock strength to the stream power, expressed in kW/m², is calculated and based on the erodibility index K .

$$P_{rock} = 0.48K^{0.44} \text{ if } K \leq 0.1$$

$$P_{rock} = K^{0.75} \text{ if } K > 0.1 \tag{5}$$

The dynamic pressure on the bottom of the stilling basin is based on two components: the mean dynamic

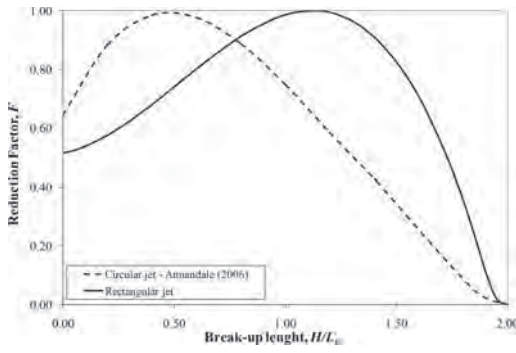


Figure 6. Reduction factor F of fluctuating dynamic pressure coefficient.

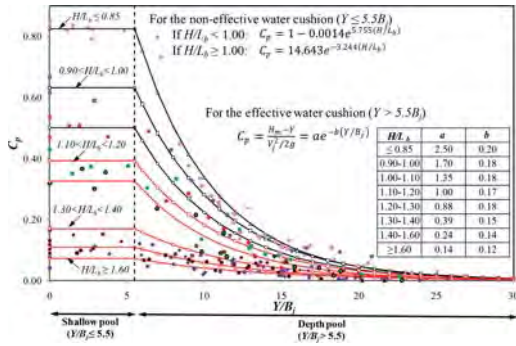


Figure 7. Mean dynamic pressure coefficient, C_p , for the nappe (rectangular) case.

pressure (C_p) and the fluctuating dynamic pressure (C'_p). These dynamic pressure coefficients are used as estimators of the stream power reduction coefficients, by an effect of the jet disintegration in the air and their diffusion in the stilling basin (Annandale, 2006). Hence, the dynamic pressures are also a function of the fall height to disintegration height ratio (H/L_b) and water cushion to impingement jet thickness (Y/B_j). The total dynamic pressure is:

$$P_{total} = C_p \left(Y/B_j \right) P_{jet} + FC'_p \left(Y/B_j \right) P_{jet} \quad (6)$$

where $C_p(Y/B_j)$ is the mean dynamic pressure coefficient, $C'_p(Y/B_j)$ the fluctuating dynamic pressure coefficient, P_{jet} the stream power per unit of area, and F the reduction factor of the fluctuating dynamic pressure coefficient.

In the rectangular jet case, Carrillo (2014) and Castillo *et al.* (2014, 2015) adjusted the formulae by using new laboratory data (Figures 6, 7 and 8).

Table 5 shows the results obtained in the three types of materials. Table 6 lists the results of incident stream (P_{jet}) and diffusion ($P_{jet}(Y/B_j)$) jet power.

Figures 9 and 10 show the stream power of the jet, together with the power threshold for the three different materials. We can observe that all flow rates impinge with enough power stream to erode a material

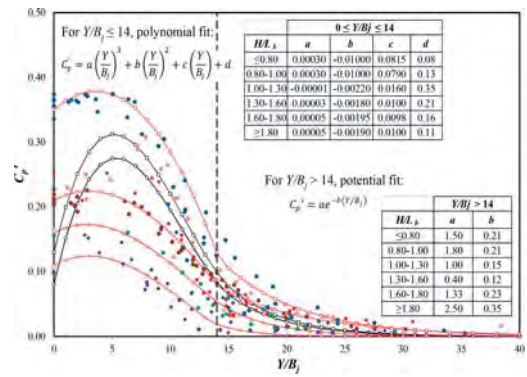


Figure 8. Fluctuating dynamic pressure coefficient, C'_p , for the nappe flow case.

Table 5. Parameters of three types of materials.

Parameters	Material Type		
	I	II	III
d_{50} (m) =	0.50	0.74	1.02
d_{84} (m) =	0.63	0.88	1.20
θ° =	32.00	33.00	34.00
M_s =	0.35	0.37	0.40
K_b =	244.14	681.47	1728.00
K_d =	0.62	0.65	0.67
J_s =	1.00	1.00	0.70
K =	53.39	163.75	326.36
P_{rock} (kW/m ²) =	19.75	45.77	76.78

Table 6. Final water cushion ($Y_0 + Y_s$), scour (Y_s), initial water cushion (Y_0), incident stream power (P_{jet}) and reduced stream power by diffusion [$P_{jet}(Y/B_j)$].

Q	$Y_0 + Y_s$ (m)	Y_s (m)	Y_0 (m)	P_{jet} (kW/m ²)	$P_{jet}(Y/B_j)$ (kW/m ²)
254	12.05	6.57	5.48	76.94	3.63
500	14.15	8.05	6.10	94.26	19.79
711	15.73	7.05	8.68	101.59	43.60
1000	17.10	7.15	9.95	113.02	71.50
1213	18.65	6.65	12.00	108.31	64.59

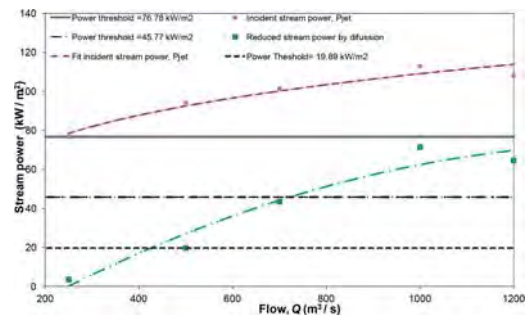


Figure 9. Incident stream power P_{jet} and reduced stream power by diffusion $P_{jet}(Y/B_j)$ of the jet. Power threshold of three types of materials (I, II, and III).

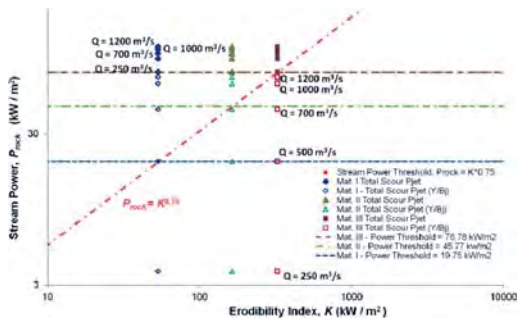


Figure 10. Stream power of the jet for different flows as a function of the erodibility. Three types of materials (I, II and III). Values ($Y_0 + Y_s$) are variables in each flow (see Table 6).

with power threshold of 76.78 kW/m^2 . However, the reduced stream power by diffusion (254 and $500 \text{ m}^3/\text{s}$), due to the effect of the water cushion ($Y_0 + Y_s$) established in the model, are below the power threshold of 19.75 kW/m^2 . The flow $711 \text{ m}^3/\text{s}$ does not have enough power to erode the material power threshold of 45.77 kW/m^2 . Flow rates of 999 and $1213 \text{ m}^3/\text{s}$ no longer have the capacity to erode the material power threshold of 76.78 kW/m^2 .

5 NUMERICAL SIMULATIONS

As a complement of the empirical and semi-empirical methodologies, three-dimensional mathematical model simulations were carried out. These programs allow a more detailed characterization than one-dimensional and two-dimensional numerical models and, thus, a detailed study of local effects of the sediments transport. The numerical simulation of the hydraulic behavior and scour by the action of the ski jump was analyzed.

The computational fluid dynamics (CFD) program FLOW-3D v11.1 was used. This program solves the Navier-Stokes equations using finite differences. It incorporates various turbulence models, a sediment transport model and an empirical model bed erosion (Guo, 2002; Mastbergen and Von den Berg, 2003; Brethour and Burnham, 2011), together with a method for calculating the free surface of the fluid without solving the air component (Hirt and Nichols, 1981). Pressures obtained in the stagnation point and their associated mean dynamic pressure coefficients were compared with the parametric methodology proposed by Castillo *et al.* (2013, 2014). This methodology was successfully used to estimate the scour downstream Paute-Cardenillo Dam (Castillo and Carrillo, 2016).

In order to simulate the proper functioning of the ski jump, several simulations were carried out by means of sensibility analysis: air entrainment models, turbulence models, grid size and type of solver, among others. Simulations were performed at laboratory scale. Multiple mesh blocks were used to solve the problem. The spillway and the ski jump were solved

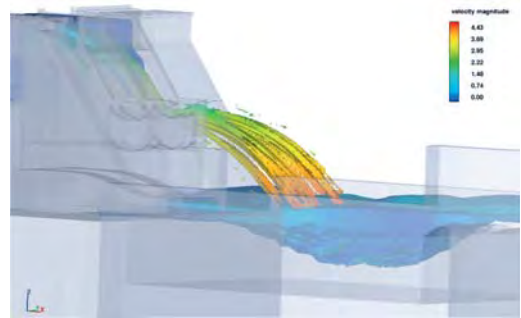


Figure 11. Numerical simulation of the scour downstream Toachi Dam.

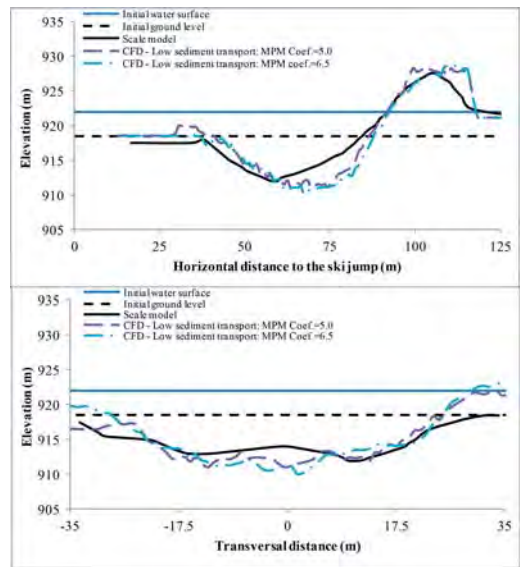


Figure 12. Longitudinal and transversal scour shape measured and simulated.

with a mesh size of 0.005 m , while the reservoir and the plunge pool were resolved with a mesh size of 0.02 m .

In the sediment scour model, the critical Shields number was calculated using Soulsby-Whitehouse equation, while the Meyer-Peter & Müller equation was used to compute the bed load transport rate. Two bed load coefficients for low sediment transport ($\beta = 5.0$ and $\beta = 6.5$) and the maximum packing fraction were used to calibrate the model.

Figure 11 shows the results obtained for the design flow ($Q = 1213 \text{ m}^3/\text{s}$) and considering a grain size of 1.00 m . The maximum scour depths were 8.50 m and 7.50 m , for β values of 6.5 and 5.0 , respectively. These values are a bit bigger than the value obtained in the physical model 6.65 m and around the mean value obtained with the empirical formulae 7.81 m .

Figure 12 compares the scour shape observed in laboratory with the numerical simulation in the planes in which the maximum scour value was measured.

The horizontal distances from the dam to the maximum scour depth were 61.50 m ($\beta = 6.5$) and 63.50 m ($\beta = 5.0$), similar to the value obtained in laboratory of 64.20 m. The longitudinal scour length from the laboratory data was around 51.55 m while the simulated value was 49 m. The transversal scour length was near the complete transversal section in both cases.

The main differences in the scour measured in laboratory and calculated seem to be related to the fact that the current version of FLOW-3D does not allow to activate the density evaluation and drift-flux models in the air entrainment model when the sediment scour model is used. This generates impact jets more compact than if the air entrainment mechanism were solved in the correct way.

6 CONCLUSIONS

In this paper, similar results have been obtained by solving the problem from four different perspectives: physical model, empirical formulations, erosion potential semi-empirical formulation and CFD simulations.

The results obtained with the reduced model and the numerical simulation with CFD, have been obtained in scale laboratory. To extrapolate to prototype, the designer should take the scale effects into account. As the air entrainment is not correctly reproduced at laboratory scales, these results are on the safe side.

The results demonstrate the suitability of crossing methodologies to solve complex phenomena. Thus, numerical simulations were used to complement the classical formulations and the laboratory results, allowing a better understanding of the physical phenomena in order to obtain an adequate solution.

ACKNOWLEDGMENTS

We are grateful to CELEC EP HIDROTOAPI for the data provided. The third author acknowledges the support of Escuela Politécnica Nacional (Ecuador) through the program Invited professor, and the support of the program PMPDI-UPCT 2015, which allowed him to develop a stay at the Centro de Investigaciones y Estudios en Recursos Hídricos CIERHI of the Escuela Politécnica Nacional (Ecuador), from September to December, 2015.

REFERENCES

- Annandale, G. W. 1995. Erodibility. *Journal of Hydraulic Research* 33 (4), 471–494.
- Annandale, G. W. 2006. *Scour Technology. Mechanics and Engineering Practice*. McGraw-Hill.
- Bisaz, E. & Tschopp, J. 1972. Profundidad de erosión al pie de un vertedero para la aplicación de corrección de arroyos en quebradas empinadas. *Proceedings of the Fifth Congreso Latinoamericano de Hidráulica (IAHR)*, Lima, Peru, 447–456 (in Portuguese).
- Bollaert, E. 2002. *Transient Water Pressures in Joint and Formations of Rock Scour due to High-Velocity Jet Impact, Communication N° 13*. Laboratory of Hydraulic Constructions, École Polytechnique Fédérale de Lausanne, Switzerland.
- Bollaert, E.F., & Schleiss, A. 2003. Scour of rock due to the impact of plunging high velocity jets. Part I: A state-of-the-art review. *Journal of Hydraulic Research* 41(5), 451–464.
- Bombardelli, F.A. & Gioia, G. 2006. Scouring of granular beds by jet-driven axisymmetric turbulent cauldrons. *Phys. Fluids* 18(8), 088–101.
- Brethour, J., & Burnham, J. 2010. Modeling Sediment Erosion and Deposition with the FLOW-3D Sedimentation & Scour Model. *Flow Science Technical Note*, FSI-10-TN85, 1–22.
- Carrillo, J. M. 2014. Metodología numérica y experimental para el diseño de los cuencos de disipación en el sobrevertido de presas de fábrica. *PhD Thesis*. Universidad Politécnica de Cartagena, Spain (in Spanish).
- Castillo, L. 1989. Metodología experimental y numérica para la caracterización del campo de presiones en los disipadores de energía hidráulica. Aplicación al vertido en presas bóveda. *PhD Thesis*. Universitat Politècnica de Catalunya. Barcelona, Spain (in Spanish).
- Castillo, L., Dolz, J. & Polo, J. 1991. Acquisition and analysis of data to characterize dynamic Actions in Hydraulic Energy Dissipators. *XXIV IAHR Congress*. D, 273–280. Madrid.
- Castillo, L. 2002. Parametrical Analysis of the Ultimate Scour and Mean Dynamic Pressures at Plunge Pools. *Workshop on Rock Scour due to High Velocity Jets*. École Polytechnique Fédérale de Lausanne.
- Castillo, L. 2006. Areated jets and pressure fluctuation in plunge pools. *The 7th International Conference on Hydroscience and Engineering (ICHE-2006)*, IAHR, ASCE, Drexel University. College of Engineering. DSpace Digital Library. DU Haggerty Library, Philadelphia, USA.
- Castillo, L., Puertas, J. & Dolz, J. 2007. Discussion about Scour of rock due to the impact of plunging high velocity jets Part I: A state-of-the-art review. *Journal of Hydraulic Research* 45 (6), 853–858.
- Castillo, L. 2007. Pressure characterization of undeveloped and developed jets in shallow and deep pool. *32nd Congress of IAHR, the International Association of Hydraulic Engineering & Research*, 2, 645–655, Venice, Italy.
- Castillo, L.G., & Carrillo, J.M. 2012. Hydrodynamics characterization in plunge pool. Simulation with CFD methodology and validation with experimental measurements. *2nd IAHR Europe Congress*, Munich.
- Castillo, L.G., & Carrillo, J.M. 2013. Analysis of the ratio scale in nappe flow case by means of CFD numerical simulations. *Proceedings of 2013 IAHR Congress*, Chengdu, China.
- Castillo, L.G., & Carrillo, J.M. 2014a. Scour analysis downstream of Paute-Cardenillo Dam. *3rd IAHR Europe Congress*, Porto.
- Castillo, L.G., Carrillo, J.M. & Sordo-Ward, A. 2014b. Simulation of overflow nappe impingement jets. *Journal of Hydroinformatics* 16(4), 922–940. DOI: 10.2166/hydro.2014.109.
- Castillo, L.G., & Carrillo, J.M. 2015a. Characterization of the dynamic actions and scour estimation downstream of a dam. *Dam Protections against Overtopping and Accidental Leakage*. CRC Press, 231–243. DOI: 10.1201/b18292–26.

- Castillo, L.G., Carrillo, J.M. & Blázquez, A. 2015b. Plunge pool dynamic pressures: A temporal analysis in the nappe flow case. *Journal of Hydraulic Research* 53(1), 101–118. DOI: 10.1080/00221686.2014.968226.
- Castillo, L.G., Carrillo, J.M. & Álvarez, M.A. 2015c. Complementary Methods for Determining the Sedimentation and Flushing in a Reservoir. *Journal of Hydraulic Engineering*, 141(11):05015004. DOI: 10.1061/(ASCE)HY.1943-7900.0001050.
- Castillo, L.G. & Carrillo. 2016. Scour, Velocities and Pressures Evaluations Produced by Spillway and Outlets of Dam. *Water*, 8 (3), 68. DOI: 10.3390/w8030068.
- Chee, S.P. & Padiyar, P.V. 1969. Erosion at the base of flip buckets. *Engineering Journal, Inst. of Canada* 52(111), 22–24.
- Ervine, D. A., & Falvey, H.R. 1987. Behavior of turbulent jets in the atmosphere and plunge pools. *Proceedings of the Institutions of Civil Engineers*, 83 (2), 295–314.
- Ervine, D. A., Falvey, H.R. & Whithers, W. 1997. Pressure Fluctuations on Plunge Pool Floors. *Journal of Hydraulic Research* 35 (2).
- Escuela Politécnica Nacional, HIDROTOAPI E.P. 2013. *Estudio experimental en modelo hidráulico. Escala 1:50. Verificación experimental del diseño definitivo de la presa Toachi y obras complementarias. Informe Técnico Fase IV.* Quito, Ecuador.
- Felderspiel, M.P. 2011. Response of an embedded block impacted by high-velocity jets. *PhD Thesis.* École Polytechnique Fédérale de Lausanne, Suisse.
- Flow Sciences Inc. 2015. *FLOW-3D Users Manual Version 11.1.* Santa Fe, New Mexico.
- Guo, J. 2002. Hunter Rouse and Shields diagram. *Proc 1th IAHR-APD Congress*, Singapore, 2, 1069–1098.
- Hartung, W. 1959. Die Kolkbildung hinter Überströmen wehren im Hinblick auf eine beweglich Sturzbettgestaltung. *Die Wasser Wirtschaft* 49(1), 309–313 (in German).
- Hidrotoapi E.P., 2010. *Informe 6256.0-R-18. Presa Toachi. Hidráulica. Memoria de cálculo.* Quito.
- Hirt, C. W. & Nichols, B. D. 1981. Volume of Fluid (VOF) Method for the Dynamics of Free Boundaries. *Journal of Computational Physics* 39 (201).
- Jaeger, C. 1939. *Über die Aehnlichkeit bei flussaulichen Modellversuchen. Wasserkraft und Wasserwirtschaft*, 34(23/24), 269 (In German).
- Machado, L.I. 1980. Formulas to calculate the scour limit on granular or rock beds. *XIII National workshop on large dams*, Subject 1, Rio de Janeiro, Brazil, 35–52.
- Martins, R. 1975. Scouring of rocky riverbeds by free-jet spillways. *Water Power & Dam Construction*. April, 1975.
- Mason, P.J. 1989. Effects of air entrainment on plunge pool scour. *Journal of Hydraulic Engineering* 115(3), 385–399.
- Mason, P.J. & Arumugan, K. 1985. Free Jets Scour below Dams and Flip Buckets, *Journal of Hydraulic Engineering* 111(2), 220–235.
- Mastbergen, D. R. & Von den Berg J. H. 2003. Breaching in fine sands and the generation of sustained turbidity currents in submarine canyons. *Sedimentology* 50, 625–637.
- Melo, J. F., Pinheiro, A. N. & Ramos, C. M. 2006. Forces on plunge pool slabs: influence of joints location and width. *Journal of Hydraulic Engineering* 132 (1), 49–60.
- Meyer-Peter, E. & Müller, R. 1948. Formulas for bed-load transport. *Proceedings of the 2nd Meeting of the International Association for Hydraulic Structures Research*, 39–64.
- Mirtskhulava, T. E. 1967. *Alguns Problemas da Erosao nos Leitos dos Rios.* Moscow. Trans. No 443do L.N.E.C. (in Portuguese).
- Puertas, J. 1994. Criterios hidráulicos para el diseño de cuencos de disipación de energía en presas bóveda con vertido libre por coronación. *PhD Thesis.* Universidad Politécnica de Cataluña, Spain (in Spanish).
- Rubinstein, G.L. 1963. Laboratory investigation of local erosion on channel beds below high overflow dams. *Transactions of Coordination Conferences on Hydraulic Engineering. Iss. VII, Conference on Hydraulics of High Head Water Discharge Structures.* Gosenergoizdat M.L.
- Taraimovich, I. I. 1978. Deformation of channels below high head spillways on rock foundations. *Hydrotechnical Construction* 9, 917–922.